Increased prefrontal activity with aging reflects nonspecific neural responses rather than compensation

Alexa M. Morcom[1]

Richard N. A. Henson[2], for Cambridge Centre for Ageing and Neuroscience[3]

[1]Centre for Cognitive Ageing and Cognitive Epidemiology, University of Edinburgh, United Kingdom

[2]MRC Cognition and Brain Sciences Unit, Cambridge CB2 3EB, United Kingdom

[3]Cambridge Centre for Ageing and Neuroscience (Cam-CAN), University of Cambridge and MRC Cognition and Brain Sciences Unit, Cambridge CB2 3EB, United Kingdom

Alexa M. Morcom can be contacted at: alexa.morcom@ed.ac.uk

No. of Figures = 3

No. of Tables = 2

No multimedia/ extended data

Abstract

Elevated prefrontal cortex activity is often observed in healthy older adults despite declines in their memory and other cognitive functions. According to one view, this activity reflects a compensatory functional posterior-to-anterior shift, which contributes to maintenance of cognitive performance when posterior cortical function is impaired. Alternatively, the increased prefrontal activity may be less specific, reflecting reduced dedifferentiation or reduced efficiency of neuronal responses due to structural and neurochemical changes accompanying aging. These accounts are difficult to distinguish on the basis of average activity levels within brain regions. Instead, we used a novel model-based multivariate analysis technique, applied to functional magnetic resonance imaging data from an adult-lifespan human sample (N=123; 66 female). Standard analysis replicated the age-related increase in average prefrontal activation during memory encoding, but multivariate tests revealed that this activity did not carry additional information. Indeed, direct tests of the relative contributions of anterior and posterior regions to memory indicated reduced reliance on prefrontal cortex with increasing age. The results contradict the posterior-to-anterior shift hypothesis, suggesting reduced specificity rather than compensation.

Significance statement

Functional brain imaging studies have often shown increased activity in prefrontal brain regions in older adults. This has been proposed to reflect a compensatory shift to greater reliance on prefrontal cortex, helping to maintain cognitive function. Alternatively, activity may become less specific as people age. This is a key question in the neuroscience of aging. In this study, we used novel tests of how different brain regions contribute to memory for events. We found increased activity in prefrontal cortex in older adults, but this activity carried less information about memory outcomes than activity in visual regions. These findings are relevant for understanding why cognitive abilities decline with age, suggesting that optimal function depends on successful brain maintenance rather than compensation.

Introduction

It is well established that healthy aging is associated with a decline in cognitive processes like memory, but mechanistic explanation of this decline is impeded by difficulties in interpreting the underlying brain changes. Functional magnetic resonance imaging (fMRI) of such cognitive processes shows striking increases, as well as decreases, in brain activity of older relative to younger adults. One leading theory – the Posterior-to-Anterior Shift in Aging (PASA) – states that compensatory recruitment of anterior regions like prefrontal cortex (PFC) contribute to maintenance of cognitive performance when posterior cortical function is impaired (Davis et al., 2008; Park and Reuter-Lorenz, 2009; Grady, 2012). Alternatively, age-related increases in PFC activity may reflect reduced specificity of neuronal responses, reflecting primary age-related changes within PFC (Park et al., 2004; Nyberg et al., 2012). It is difficult to adjudicate between these theories based on average activity levels within brain regions (Morcom and Johnson, 2015). We used a novel multivariate approach to directly test predictions of the PASA theory.

With multivariate methods that examine distributed patterns of brain activity over many voxels, one can ask whether increased anterior activity provides additional information, beyond that carried by posterior cortical regions. Such complementary information would support theories like PASA that attribute additional PFC recruitment to compensatory mechanisms. We used a model-based decoding approach called multivariate Bayes (MVB) (Friston et al., 2008; Morcom and Friston, 2012; Chadwick et al., 2014), which estimates the patterns of activity that best predict a target cognitive outcome. Importantly, MVB allows formal comparison of models comprising different brain regions, such as PFC, posterior cortex, or their combination.

In this study, we applied MVB to fMRI data from a memory encoding paradigm in a population-derived, adult-lifespan sample (N=123, 19-88 years; Shafto et al. 2014). Participants were scanned while encoding new memories of unique pairings of objects and background scenes, and the target cognitive outcome was whether or not these associations were subsequently remembered (Fig 1). A previous behavioral study in an independent sample showed a strong decline in such associative memory across the adult lifespan (Henson et al., 2016). We defined two regions-of-interest (ROIs): posterior visual cortex (PVC), comprising lateral occipital and fusiform cortex, and PFC, comprising ventrolateral, dorsolateral, superior and anterior regions (Fig 2a). These ROIs were based on previous fMRI studies of memory encoding, and those cited in the context of the PASA theory (Davis et al., 2008; Maillet and Rajah, 2014).

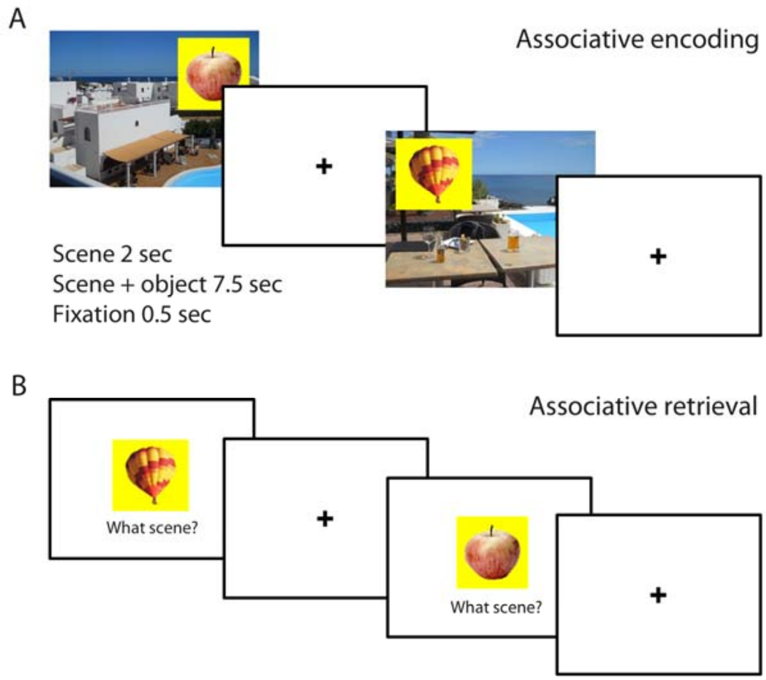

Figure 1. Associative encoding task. In the scanned Study phase, participants were asked to make up a story that linked each object with its background scene (120 trials total). On each trial, the scene was presented for 2 sec, then the object superimposed for 7.5 sec, finally the screen was blanked for 0.5 sec before the next trial. At Test (out of the scanner), each object was presented again, and after a measure of priming, item memory and background valence memory, participants were asked to verbally describe the scene with which it was paired at Study. The latter verbal recall was scored as correct or incorrect, which was then used to classify the trials at Study into "remembered" and "forgotten" (see text for details).

Materials and Methods

Participants

A healthy, population-derived adult lifespan human sample (N=123; 19-88 years; 66 female) was collected as part of the Cam-CAN study(Shafto et al., 2014). Participants were fluent English speakers in good physical and mental health. Exclusion criteria included a low Mini Mental State Examination (MMSE) score (<=24), serious current medical or psychiatric problems, or poor hearing or vision, as well as standard MRI safety criteria. Two participants were excluded from the current analysis as subsequent memory could not successfully be decoded from either region of interest (see Multivariate Bayesian decoding). Two further participants were excluded because of statistical outlier values in the analysis of univariate subsequent memory effects (see Statistics for criteria). The experiment used a within-participant design, so all participants received all the task conditions. Therefore, randomization and blinding were not required. The study was approved by the Cambridgeshire 2 (now East of England—Cambridge Central) Research Ethics Committee. Participants gave informed written consent.

Materials

Stimuli were 160 pictures of everyday emotionally-neutral objects taken from(Smith et al., 2004). For the study phase, objects were presented within a square yellow background on one of 120 scenes from the IAPS emotional pictures database(Lang et al., 1997). Scenes were grouped into 40 per valence (positive, neutral, negative), selected based on a pilot study, with the same randomized trial order for each valence condition for all participants. To control for stimulus effects, the 160 objects were divided randomly into 4 sets, and the allocation of object sets to scene valence rotated across participants in 4 different counterbalances (see (Henson et al., 2016) for further details).

Behavioral procedure

The behavioural paradigm is summarized in Figure 1. The scanned study phase comprised 120 trials, presented in two 10 min blocks separated by a short break. On each study trial, a background scene was first presented for 2 sec, and an object then superimposed for 7.5 sec, slightly above center and either to the left or right. Participants were asked to create a story that linked the object to the scene, to press a button when they had made the story, and to continue to elaborate it until the scene and object disappeared. A blank screen of 0.5 sec was then presented prior to the next trial. Participants were informed that the task would include some pleasant and unpleasant scenes. They were not told that their memory would be tested later. A practice session of 6 study trials was given just beforehand.

The test phase took place outside the scanner, following a short break of approximately 10 min involving refreshment and conversation with the experimenter. The 120 objects from the study phase were presented again, randomly intermixed with 40 new objects, and divided into 4 blocks lasting approximately 20 min each. The first stage of each test involved a priming measure: the masked version of the object was presented in the center of the screen, and participants were asked to identify it, making a keypress response and at the same time either naming the object aloud or saying “don’t know”. Next, item memory was tested by removing the pixel-noise and asking participants to judge whether the object had appeared in the study phase and to indicate their level of confidence in this judgement by pressing one of four keys: “sure new”, “think new”, “think studied”, “sure studied”. They were told that about one quarter of objects were new. Associative memory was then tested for all items judged "studied" ("think" or "sure"), by asking participants to state aloud the type of background the object had been studied with (positive, neutral, or negative, or "don't know").

Lastly, and relevant to the present study, participants were asked to verbally describe the scene that had been paired with the test object at study. Trials at study in which scenes that were correctly recalled at test, in terms of detail or gist, were scored as "remembered", whereas study trials for which the scenes could not be recalled, or for which an incorrect scenes was described instead, or for which the object was not recognised, were scored as "forgotten". Split by age tertile, the mean numbers of trials (SD) for Remembered and Forgotten trials were 55 (25) and 65 (25) for young adults (19-45 years; n=38), 44 (24) and 76 (24) for middle aged adults (46-64 years; n=43), and 23 (15) and 97 (15) for older adults (65-88 years; n=42).

As expected, regression against age showed that the number of remembered trials decreased with age (linear $t(120)=-8.06$, $P<.001$; with no significant quadratic component, $t(120)=-0.50$, $P=.62$)); two-tailed tests.

Imaging data acquisition and preprocessing

The MRI data were collected using a Siemens 3 T TIM TRIO system (Siemens, Erlangen, Germany). MR data preprocessing and univariate analysis used the SPM12 software (Wellcome Department of Imaging Neuroscience, London, UK, www.fil.ion.ucl.ac.uk/spm), release 4537, implemented in the AA 4.0 pipeline (https://github.com/rhodricusack/automaticanalysis).

The functional images were acquired using T2*-weighted data from a Gradient-Echo Echo-Planar Imaging (EPI) sequence. A total of 320 volumes were acquired in each of the 2 Study sessions, each containing 32 axial slices (acquired in descending order), slice thickness of 3.7 mm with an interslice gap of 20% (for whole brain coverage including cerebellum; TR =1970 milliseconds; TE =30 milliseconds; flip angle =78 degrees; FOV =192 mm × 192 mm; voxel-size =3 mm × 3 mm × 4.44 mm). A structural image was also acquired with a T1-weighted 3D Magnetization Prepared RApid Gradient Echo (MPRAGE) sequence (repetition time (TR) 2250ms, echo time (TE) 2.98 ms, inversion time (TI) 900 ms, 190 Hz per pixel; flip angle 9 deg; field of view (FOV) 256 x 240 x 192 mm; GRAPPA acceleration factor 2).

The structural images were rigid-body registered with an MNI template brain, bias-corrected, segmented and warped to match a gray-matter template created from the whole CamCAN Stage 3 sample (N=272) using DARTEL (Ashburner, 2007) (see Taylor *et al.*, 2015) for more details). This template was subsequently affine-transformed to standard Montreal Neurological Institute (MNI) space. The functional images were then spatially realigned, interpolated in time to correct for the different slice acquisition times, rigid-body coregistered to the structural image and then transformed to MNI space using the warps and affine transforms from the structural image, and resliced to 3x3x3mm voxels.

Regions of interest (ROIs)

ROIs were defined using WFU PickAtlas (http://fmri.wfubmc.edu/, version 3.0.5) with AAL and Talairach atlases (Lancaster et al., 2000; Tzourio-Mazoyer et al., 2002; Maldjian et al., 2003). The posterior visual cortex (PVC) mask comprised bilateral lateral occipital cortex and fusiform cortex (from AAL, fusiform and middle occipital gyri), and the PFC mask comprised bilateral ventrolateral, dorsolateral, superior and anterior regions (from AAL, the inferior frontal gyrus, both pars triangularis and pars orbitalis; middle frontal gyrus, lateral part; superior frontal gyrus, medial part; and from Talairach, Brodmann Area 10, dilation factor = 1).

Univariate imaging analysis

For each participant, a General Linear Model (GLM) was constructed, comprising three neural components per trial: 1) a delta function at onset of the background scene, 2) an epoch of 7.5 seconds which onset with the appearance of the object (2s after onset of scene) and offset when both object and scene disappeared, and 3) a delta function for each keypress. Each neural component was convolved with a canonical haemodynamic response function (HRF) to create a regressor in the GLM. The scene onset events were split into three types (i.e, three regressors) according to the valence of the scene on each trial, while the keypress events were modelled by the same regressor for all trials (together, these four regressors served to model trial-locked responses that were not of interest). The responses of interest were captured by the epoch neural component, during which participants were actively relating the scene and object (see Behavioral Procedure). This epoch component was split into 6 types (regressors) according to the three scene valences and the two types of subsequent memory. Six additional regressors representing the 3 rigid body translations and rotations estimated in the realignment stage were included to capture residual movement-related artifacts. Finally the data were scaled to a grand mean of 100 over all voxels and scans within a session.

The GLM was fit to the data in each voxel. The autocorrelation of the error was estimated using an AR(1)-plus-white-noise model, together with a set of cosines that functioned to highpass the model and data to 1/128 Hz, fit using Restricted Maximum Likelihood (ReML). The estimated error autocorrelation was then used to “prewhiten” the model and data, and ordinary least squares used to estimate the model parameters. To compute subsequent memory effects, the parameter estimates for the 6 epoch components were averaged across the two sessions and the three valences (weighted by number of trials per session/valence), and contrasted directly as remembered minus forgotten (Morcom et al., 2003; Maillet and Rajah, 2014). Univariate statistical analyses were conducted on the mean subsequent memory effect across all voxels in the MVB analysis, in each ROI for each participant (see next section).

Multivariate Bayesian decoding

A series of MVB decoding models were fit to assess the information about subsequent memory carried by individual ROIs or combinations of ROIs. MVB estimates the free energy, which provides an upper bound on the Bayesian log-evidence. The evidence for different models can then be compared, or the fitted model weights examined to assess their distribution over voxels and the contributions of different voxels. These analyses were implemented in SPM12 v6486 and custom MATLAB scripts.

MVB maps many physiological data features (the predictor variables are formed from fMRI activity in multiple voxels) to a psychological target variable. Each MVB decoding model is based on the same design matrix of experimental variables used in the above univariate GLM. The target variable is specified as a contrast, in this case subsequent memory. Modelled confounds in the design (all covariates apart from those involved in the target contrast) are removed from both target and predictor variables. Each MVB model is fit using hierarchal parametric empirical Bayes, specifying empirical priors on the data features (voxel-wise activity) in terms of patterns over voxel features and the variances of the pattern weights. Since decoding models operating on multiple voxels (relative to scans) are ill-posed, these priors on the patterns of voxel weights act as constraints in the second level of the hierarchical model. MVB also uses an overall sparsity (hyper) prior in pattern space which embodies the expectation that a few patterns make a substantial contribution to the decoding and most make a small contribution. The pattern weights specifying the mapping of data features to the target variable are optimised with a greedy search algorithm using a standard variational scheme (Friston et al., 2007). In this work we used a sparse spatial prior, in which each pattern is an individual voxel (Morcom and Friston, 2012; Chadwick et al., 2014; Hulme et al., 2014; Maass et al., 2014) (log evidence was substantially greater for sparse than spatially smooth priors in both ROIs: for 1-tailed t-tests comparing to population mean=3, in PVC, $t=4.65$, $p<.001$ and PFC, $t=6.91$, $p<.001$, $n=119$).

Features (voxels) for MVB analysis were selected using an orthogonal contrast and a leave-one-participant-out scheme. For each participant and ROI, these were the 1000 voxels with the strongest responses to the 6 epoch regressors in the above GLM (defined using an F contrast in all other participants testing variance explained by these regressors, regardless of valence or subsequent memory). We then checked that subsequent memory could reliably be decoded from the selected features by contrasting the evidence for each model with the evidence for models in which the design matrix (and therefore the target variable) had been randomly phase-shuffled, taking the mean over 20 repetitions. This difference in log-evidence corresponds to the log (marginal) likelihood ratio or log Bayes factor for comparing the real and phase-shuffled models. Log evidence was robustly greater for real than shuffled models in both PVC (t=7.96, p<.0001, mean difference = 12.7, SE=1.60; two-tailed, n=119) and PFC (t=10.5, p<.0001, mean difference = 18.7, SE=1.78; two-tailed, n=119).

Unlike univariate activation measures such as subsequent memory effects, but like other pattern-information methods, MVB finds the best non-directional model of activity predicting the target variable, so positive and negative pattern weights are equally important. Therefore, the principle MVB measure of interest for each ROI was the spread (standard deviation) of the weights over voxels, reflecting the degree to which multiple voxels carried substantial information about subsequent memory. We also constructed two novel measures of the contribution of prefrontal cortex to subsequent memory. The first used Bayesian model comparison within participants to test whether a joint PVC-PFC model boosted prediction of subsequent memory relative to a PVC-only model. The PASA hypothesis, in which PFC is engaged to a greater degree in older age and this contributes to cognitive outcomes, predicts that a boost will be more often observed with increasing age. The initial dependent measure was the log model evidence, coded categorically for each participant to indicate the outcome of the model comparison. The 3 possible outcomes were: a boost to model evidence for PVC-PFC relative to PVC models, i.e., better prediction of subsequent memory (difference in log evidence > 3), equivalent evidence for the two models (-3 < difference in log evidence < 3), or a reduction in prediction of subsequent memory for PFC-PVC relative to PVC (difference in log evidence < -3). The second novel measure of PFC contribution to subsequent memory was the proportion of top-weighted voxels in the joint PVC-PFC model that were located in PFC, as opposed to PVC, derived from joint PVC-PFC models. In each participant, the voxels making the strongest contribution to subsequent memory, defined as those with absolute voxel weight values greater than 2 standard deviations from the mean, were divided according to their anterior versus posterior location. The dependent measure was the proportion of these top voxels located in PFC.

Experimental design and statistical analysis

Sample size was determined by the initial considerations of Stage 3 of the CamCAN study – see Shafto et al.(Shafto et al., 2014) for details. For this secondary data analysis study, a sensitivity analysis indicated that with N=123, we would have 80% power to detect a small to medium effect explaining 7.4% of the variance (r^2=.074). In our previous report of aging and successful memory encoding, an *a priori* test of a between-region difference in subsequent memory effects according to age showed a large effect (r^2=.257) (Morcom et al., 2003).

Age effects on continuous multivariate or univariate dependent measures were tested using robust second-order polynomial regression with "rlm" in the package MASS for R (Venables et al., 2002); MASS version 7.3-45; R version 3.3.1) and standardized linear and quadratic age predictors. Analysis of outcomes of the between-region MVB model comparison (PVC and PFC combined versus PVC, see Fig 2 and main text) used ordinal regression with "polr" in MASS. Distributions were also trimmed to remove extreme outliers (> 5 SD above or below the mean). The two participants (aged 72 and 80) with outlier values for univariate effects were also removed from the MVB analyses so the samples examined were comparable. Finally, we excluded two further participants (aged 68 and 83) in whom subsequent memory could not be decoded from at least one of the two ROIs (log model evidence <= 3), giving n=119. All tests were two-tailed and used an alpha level of .05.

Where it was important to test for evidence for the null hypothesis over an alternative hypothesis, we supplemented null-hypothesis significance tests with Bayes Factors (Wagenmakers, 2007; Rouder et al., 2009). The Bayes Factors were estimated using Dienes' online calculator (Dienes, 2014) which operationalizes directional hypotheses such as PASA in terms of a half-normal distribution. Here, as the regression betas were standardized, the half-normal distribution had mean=0 and SD=1.

Results

Standard univariate activation analyses assessed mean activity in each ROI across all voxels included in the multivariate analysis (see Materials and Methods). These confirmed that activity in both ROIs positively predicted subsequent memory across the lifespan (PVC: $t(118) = 4.42$, $p < .001$; PFC: $t(118) = 2.13$, $p = .035$). Consistent with the PASA account, PFC activity increases for subsequently remembered versus forgotten items also became more pronounced with age, particularly in later years (for linear effect of age, $t(118) = 2.43$, $p=.017$; for quadratic effect of age, $t(118) = 2.58$, $p = .012$) (Fig 2b). Age effects in PVC were not significant, though there was also no evidence that age effects in the two ROIs differed (see Table 1).

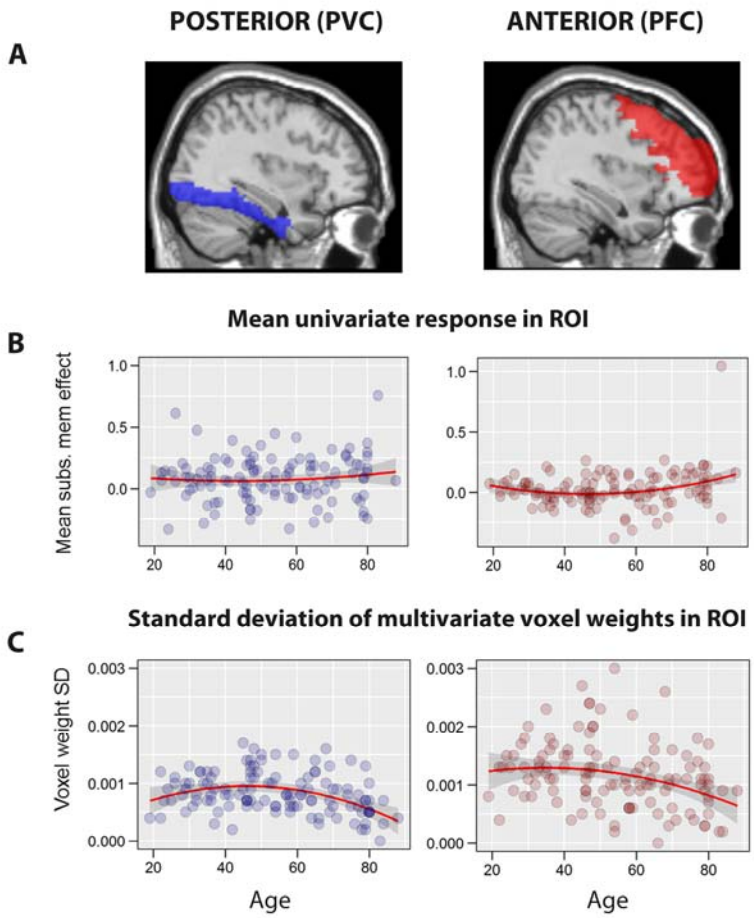

Figure 2. Relationship between age and subsequent memory effects within ROIs. **(a)** PVC (blue) and PFC (red) ROIs overlaid on sagittal section (x=+36) of a canonical T1 weighted brain image. **(b)**. Univariate subsequent memory effects (mean activity for remembered - forgotten), showing increased activity with age in PFC but not PVC. (c). Spread of multivariate responses predicting subsequent memory (standard deviation of fitted MVB voxel weights), showing reduced spread of responses with age in both ROIs. Red and blue lines are robust-fitted second-order polynomial regression lines and shaded areas show 95% confidence intervals.

ROI/ measure		**Linear**			**Quadratic**	
	t	R^2_{adj}	p	*t*	R	P
Mean						
PVC	0.728	--	0.480	0.703	--	0.495
PFC	2.43	.032	0.017	2.58	.038	0.012
PFC-PFC	0.883	--	0.388	1.084	--	0.293
SD						

PVC	5.91	.216	< .0001	1.72	--	0.093
PFC	5.64	.200	< .0001	0.747	--	0.460
PFC-PFC	-5.51	.192	< .0001	-2.31	.027	0.024

Table 1. Age effects on mean and standard deviation of univariate SM effects. SD = standard deviation. n=119. R^2_{adj} = the unbiased estimate of the amount of variance explained in the population.

If the increased activation in PFC reflected a compensatory PASA shift, we expected the multivariate analyses to show that this increased activity carried additional information about subsequent memory. However, the data revealed a different pattern. In MVB models, like other linear models with multiple predictors, each voxel within an ROI has a weight which captures the unique information it contributes (in this case, for predicting subsequent memory). Because both positive and negative weights carry information, we summarised the MVB results by the spread (standard deviation) of weights over voxels (see Materials and Methods).

In both ROIs, this spread was markedly reduced during later life (PVC: for linear effect of age, $t(118) = -3.49$, $p < .001$; for quadratic effect of age, $t(118) = 3.50$, $p < .001$; PFC: linear $t(118) = -3. 34$, $p < .001$; quadratic $t(118) = -1.44$, $p = .151$) (see Fig 2c and Table 2). This means that, contrary to a compensatory PASA shift, PFC showed fewer, rather than more, voxels with large positive or negative weights with increasing age. Moreover, direct comparison across ROIs showed that the age-related reduction in spread of weights was greater in PFC than PVC (linear $t(118) = -2.02$, $p = .044$). By contrast, the spread of univariate activities across voxels increased with age in both ROIs (Table 1).

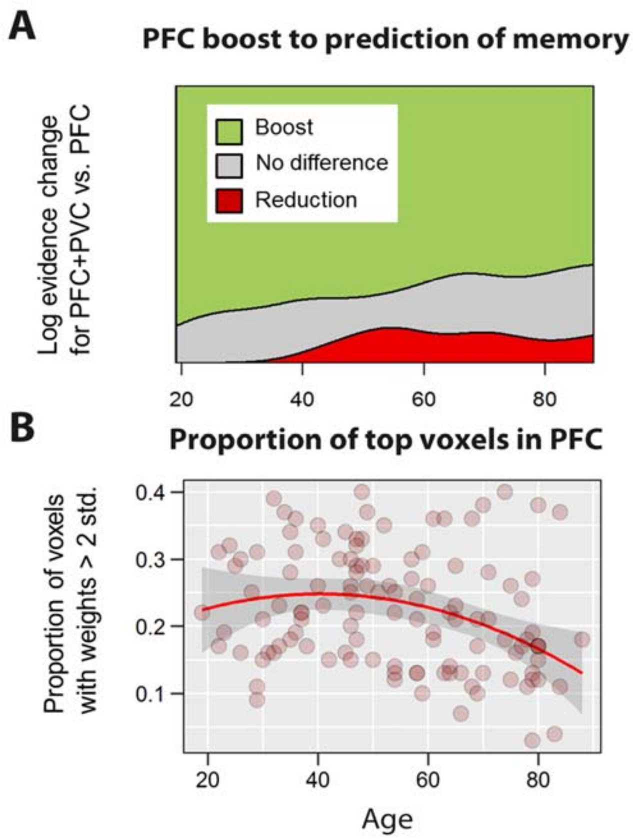

Figure 3. Evidence against a posterior-to-anterior shift from MVB comparisons between ROIs. **(a)** Ordinal regression of Bayesian model comparison of combined PVC-PFC model versus PVC-only model showed that a boost (difference in log-evidence > 3) for the combined model relative to the PVC model was no more frequent with increasing age relative to no boost (-3 < difference < 3) or a reduction (difference < -3). **(b)** The proportion of top-weighted voxels (> 2 standard deviations above mean) that fell within PFC (rather than PVC) showed an age-related reduction. The red line is a robust-fitted second-order polynomial regression line and the shaded area shows 95% confidence intervals.

ROI/ measure	**Linear**			**Quadratic**		
	t	r	p	*T*	r	p
Mean						
PVC	-2.06	.187	.039	2.23	.202	.026
PFC	-.338	--	.732	1.88	--	.059
PFC-PFC	1.09	--	.278	-.196	--	.844
SD						

PVC	-3.49	.307	<.001	-3.50	.308	<.001
PFC	-3.33	.294	.001	-1.44	--	.151
PFC-PFC	-2.02	.184	.044	.398	--	.690

Table 2. Age effects on mean and standard deviation of MVB voxel weights. SD = standard deviation. n=119.

To provide more direct tests for a posterior-to-anterior shift, we developed two measures of the relative contribution of PFC and PVC to subsequent memory after fitting joint MVB models that included both posterior and anterior ROIs. First, we used Bayesian model comparison in each participant to test whether adding PFC to the model – the joint PVC-PFC model – "boosted" prediction of subsequent memory relative to the PVC-only model (see Methods). Contrary to the PASA theory of a compensatory shift to greater reliance on PFC, a Bayes Factor comparing these two models revealed strong evidence for the null hypothesis of no boost (BF = 11.1); indeed, the probability of a boost to model evidence for PVC-PFC compared to PVC-only actually *decreased* with age numerically (Fig 3a; linear $t(118) = -1.54$, $p = .064$). Second, we measured the proportion of top-weighted voxels (> 2 standard deviations above the mean) in the joint PVC-PFC model that were located in PFC, as opposed to in PVC. However, this proportion significantly *decreased* with age (Fig 3b; linear $t(118) = -3.31$, $p = .00132$; quadratic $t(118) = -1.99$, $p = .0490$), again contrary to PASA.

Discussion

This study investigated the proposal that there is a posterior-to-anterior shift in task-related brain activity during aging, with a greater relative reliance on prefrontal cortex in older age. We tested predictions of this PASA theory with data from an episodic memory encoding task that was conducted on a relatively large population-derived adult lifespan sample. Using novel model-based multivariate analyses, we provide direct evidence against a posterior-to-anterior shift. Instead, our data suggest that increased PFC activity in older adults was less specific rather than compensatory, and that older adults relied *less* on prefrontal relative to posterior areas.

The results of the standard univariate activation analyses are consistent with previous studies showing age-related increases in activation in prefrontal cortex, which form the basis of the PASA theory (Grady et al., 1994; Davis et al., 2008). The increase was relatively modest, but generalizes previous findings in that it was reliable across lateral, anterior and superior areas. Despite this, multivariate analysis showed that with increasing age, fewer voxels in each ROI strongly predicted subsequent memory. This negative effect of age on the spread of multivariate responses was accompanied by a positive effect on the spread of univariate activation responses across voxels. This, suggests that, while more voxels showed substantial (positive or negative) responses related to subsequent memory in older people, these additional responses were redundant, with fewer voxels contributing uniquely to memory encoding, as expected if increased prefrontal activity is less specific.

The notion of a posterior-to-anterior shift implies an age-related increase in PFC activity *relative* to posterior activity (Morcom and Johnson, 2015). Direct comparisons have not generally been made, but evidence for a shift comes from findings of cross-over effects in which age-related decreases in posterior cortical activity occur alongside age-related increases in PFC (e.g., Grady et al., 1994; Davis et al., 2008). Numerous other studies have focused on age-related increases in PFC rather than a shift relative from posterior cortex (e.g., Cabeza et al., 1997; Anderson et al., 2000). A recent meta-analysis of subsequent memory effects supported PASA, with age-related increases in older adults in several PFC regions (Maillet and Rajah, 2014), and decreases in PVC, although another meta-analysis across different tasks found age-related decreases as well as increases in different PFC regions (Spreng et al., 2010). In individual studies, neighbouring areas of PVC (Grady et al., 1994) and PFC (Rajah and D'Esposito, 2005) can also show both age-related increases and decreases. A strength of our approach is that our multivariate analyses encompassed large ROIs in both anterior and posterior cortices, as well as direct comparisons between the two.

The univariate activation analyses showed no evidence of a posterior-to-anterior shift, as age effects in PFC and PVC did not differ. However, the reduction in multivariate responses predicting subsequent memory was more pronounced in PFC than PVC. Together with the evidence that the activity was less specific, this implicates age-related effects in both regions which impact PFC to a greater degree, consistent with evidence from structural studies (West, 1996; Raz and Rodrigue, 2006). One mechanism by which deleterious changes can give rise to increased activity may be a pervasive dedifferentiation of neuronal representations, which predominantly affects complex cognitive functions (Li et al., 2001; Park et al., 2004; Carp et al., 2011; Abdulrahman et al., 2014). Alternatively, processing may become less efficient, providing less computational "bang for the buck" for the same level of neural activity (Rypma and Esposito, 2000; Morcom et al., 2007; Grady, 2008; Reuter-Lorenz and Campbell, 2008; Nyberg et al., 2014). According to these theories, increased activation in older adults reflects loss of neuronal integrity rather than compensation.

The PASA theory proposes that PFC is not only engaged to a greater degree in older adults but that the additional activity also compensates, i.e., helps to maintain cognitive function. Unique insights are therefore to be gained from joint analysis of the contributions of anterior and posterior regions. Using multivariate models of both PFC and PVC, we constructed two novel measures of the degree to which unique information about subsequent memory was carried by PFC: 1) A direct model comparison showed that PFC did not contribute more to subsequent memory with increasing age, over and above the contribution of PVC, while a direct comparison of the number of influential voxels failed to support the hypothesis that PFC plays a stronger role with increasing age. On the contrary, we found that fewer of the voxels most strongly predicting subsequent memory were located in PFC relative to PVC in older adults.

Our data replicate a (modest) increase in PFC activity over the adult lifespan, but do not support the idea that this reflects a compensatory posterior-to-anterior shift, at least in the context of memory encoding. The results are most parsimoniously explained by reduced specificity of neural responses reflecting primary age-related deleterious changes leading to dedifferentiation or inefficient neural computation. Our results therefore help to adjudicate between two main competing accounts of neurocognitive aging, while also illustrating the ability of MVB to compare models that comprise different sets of voxels, thereby offering an exciting new general way to test the relative contributions of brain regions to cognitive outcomes.

Acknowledgments

A.M.M. is a member of the University of Edinburgh Centre for Cognitive Ageing and Cognitive Epidemiology (CCACE), part of the UK cross-council Lifelong Health and Wellbeing Initiative, Grant number G0700704/84698. The Cambridge Centre for Ageing and Neuroscience (Cam-CAN) research was supported by the Biotechnology and Biological Sciences Research Council (grant number BB/H008217/1). The full Cam-CAN author list can be found here: http://www.cam-can.org/index.php?content=corpauth. R.N.A.H. is funded by the Medical Research Council (MC_A060_5PR10).

Author contributions

A.M.M. and R.N.A.H. designed research; A.M.M., R.N.A.H. and Cam-CAN performed research; A.M.M. and R.N.A.H. analyzed data; A.M.M. and R.N.A.H. wrote the paper.

References

Abdulrahman H, Fletcher PC, Bullmore E, Morcom AM (2014) Dopamine and memory dedifferentiation in aging. Neuroimage.

Anderson ND, Iidaka T, Cabeza R, Kapur S, McIntosh a R, Craik FI (2000) The effects of divided attention on encoding- and retrieval-related brain activity: A PET study of younger and older adults. J Cogn Neurosci 12:775–792.

Ashburner J (2007) A fast diffeomorphic image registration algorithm. 38:95–113.

Cabeza R, McIntosh AR, Tulving E, Nyberg L, Grady CL (1997) Age-related differences in effective neural connectivity during encoding and recall. Neuroreport 8:3479–3483 Available at: http://www.biomednet.com/db/medline/98087183%5Cnhttp://graphics.tx.ovid.com/ovftpdfs/FPDDNCOBFAOJIC00/fs041/ovft/live/gv012/00001756/00001756-199711100-00013.pdf.

Carp J, Park J, Polk TA, Park DC (2011) Age differences in neural distinctiveness revealed by multi-voxel pattern analysis. Neuroimage 56:736–743 Available at: http://dx.doi.org/10.1016/j.neuroimage.2010.04.267.

Chadwick MJ, Bonnici HM, Maguire E a. (2014) CA3 size predicts the precision of memory recall. Proc Natl Acad Sci 111:10720–10725 Available at: http://www.pubmedcentral.nih.gov/articlerender.fcgi?artid=4115494&tool=pmcentrez&rendertype=abstract.

Davis SW, Dennis NA, Daselaar SM, Fleck MS, Cabeza R (2008) Que PASA? the posterior-anterior shift in aging. Cereb Cortex 18:1201–1209.

Dienes Z (2014) Using Bayes to get the most out of non-significant results. Front Psychol 5:1–17.

Friston K, Chu C, Mour??o-Miranda J, Hulme O, Rees G, Penny W, Ashburner J (2008) Bayesian decoding of brain images. Neuroimage 39:181–205.

Friston K, Mattout J, Trujillo-Barreto N, Ashburner J, Penny W (2007) Variational free energy and the Laplace approximation. Neuroimage 34:220–234.

Grady C (2012) The cognitive neuroscience of ageing. Nat Rev Neurosci 13:491–505 Available at: http://www.ncbi.nlm.nih.gov/pubmed/22714020.

Grady CL (2008) Cognitive neuroscience of aging. Ann N Y Acad Sci 1124:127–144.

Grady CL, Maisog JM, Horwitz B, Ungerleider LG, Mentis MJ, Salerno JA, Pietrini P, Wagner E, Haxby J V (1994) Age-related changes in cortical blood flow activation during visual processing of faces and location. J Neurosci 14:1450–1462.

Henson RN et al. (2016) Multiple determinants of lifespan memory differences. Sci Rep 6:32527 Available at: http://www.nature.com/articles/srep32527.

Hulme OJ, Skov M, Chadwick MJ, Siebner HR, Rams??y TZ (2014) Sparse encoding of automatic visual association in hippocampal networks. Neuroimage 102:458–464 Available at: http://dx.doi.org/10.1016/j.neuroimage.2014.07.020.

Lancaster JL, Woldorff MG, Parsons LM, Liotti M, Freitas CS, Rainey L, Kochunov P V., Nickerson D, Mikiten SA, Fox PT (2000) Automated Talairach Atlas labels for functional brain mapping. Hum Brain Mapp 10:120–131.

Lang PJ, Bradley MM, Cuthbert BN (1997) International Affective Picture System (IAPS): Technical Manual and Affective Ratings. NIMH Cent Study Emot Atten:39–58 Available at: http://www.unifesp.br/dpsicobio/adap/instructions.pdf%5Cnhttp://econtent.hogrefe.com/

doi/abs/10.1027/0269-8803/a000147.

Li S-C, Li S-C, Lindenberger U, Lindenberger U, Sikstrom S, Sikstrom S (2001) Aging cognittion: From neuromodulation to representation. 5:479–486.

Maass A, Schütze H, Speck O, Yonelinas A, Tempelmann C, Heinze H-J, Berron D, Cardenas-Blanco A, Brodersen KH, Enno Stephan K, Düzel E (2014) Laminar activity in the hippocampus and entorhinal cortex related to novelty and episodic encoding. Nat Commun 5:5547 Available at: http://www.nature.com/doifinder/10.1038/ncomms6547%5Cnhttp://www.pubmedcentral.nih.gov/articlerender.fcgi?artid=4263140&tool=pmcentrez&rendertype=abstract.

Maillet D, Rajah MN (2014) Age-related differences in brain activity in the subsequent memory paradigm: A meta-analysis. Neurosci Biobehav Rev 45:246–257 Available at: http://dx.doi.org/10.1016/j.neubiorev.2014.06.006.

Maldjian JA, Laurienti PJ, Kraft RA, Burdette JH (2003) An automated method for neuroanatomic and cytoarchitectonic atlas-based interrogation of fMRI data sets. Neuroimage 19:1233–1239.

Morcom AM, Friston KJ (2012) Decoding episodic memory in ageing: A Bayesian analysis of activity patterns predicting memory. Neuroimage 59.

Morcom AM, Good CD, Frackowiak RSJ, Rugg MD (2003) Age effects on the neural correlates of successful memory encoding. Brain 126.

Morcom AM, Johnson W (2015) Neural reorganization and compensation in aging. J Cogn Neurosci 27.

Morcom AM, Li J, Rugg MD (2007) Age effects on the neural correlates of episodic retrieval: Increased cortical recruitment with matched performance. Cereb Cortex 17.

Nyberg L, Andersson M, Kauppi K, Lundquist A, Persson J, Pudas S, Nilsson LG (2014) Age-related and genetic modulation of frontal cortex efficiency. J Cogn Neurosci 26:746–764.

Nyberg L, L??vd??n M, Riklund K, Lindenberger U, B??ckman L (2012) Memory aging and brain maintenance. Trends Cogn Sci 16:292–305.

Park DC, Polk TA, Park R, Minear M, Savage A, Smith MR (2004) Aging reduces neural specialization in ventral visual cortex. 101:13091–13095.

Park DC, Reuter-Lorenz P (2009) The adaptive brain: aging and neurocognitive scaffolding. Annu Rev Psychol 60:173–196 Available at: http://www.ncbi.nlm.nih.gov/pubmed/19035823.

Rajah MN, D'Esposito M (2005) Region-specific changes in prefrontal function with age: A review of PET and fMRI studies on working and episodic memory. Brain 128:1964–1983.

Raz N, Rodrigue KM (2006) Differential aging of the brain: Patterns, cognitive correlates and modifiers. Neurosci Biobehav Rev 30:730–748.

Reuter-Lorenz PA, Campbell KA (2008) Neurocognitive ageing and the Compensation Hypothesis. Curr Dir Psychol Sci 17:177–182.

Rouder JN, Speckman PL, Sun D, Morey RD, Iverson G (2009) Bayesian t tests for accepting and rejecting the null hypothesis. Psychon Bull Rev 16:225–237.

Rypma B, Esposito MD (2000) Isolating the neural mechanisms of age-related changes in human working memory. 3:509–515.

Shafto M a, Tyler LK, Dixon M, Taylor JR, Rowe JB, Cusack R, Calder AJ, Marslen-Wilson WD, Duncan J, Dalgleish T, Henson RN, Brayne C, Matthews FE (2014) The Cambridge Centre for Ageing and Neuroscience (Cam-CAN) study protocol: a cross-sectional, lifespan, multidisciplinary examination of healthy cognitive ageing. BMC Neurol 14:204 Available at: http://www.pubmedcentral.nih.gov/articlerender.fcgi?artid=4219118&tool=pmcentrez&rendertype=abstract.

Smith APR, Henson RNA, Dolan RJ, Rugg MD (2004) fMRI correlates of the episodic retrieval of emotional contexts. Neuroimage 22:868–878.

Spreng RN, Wojtowicz M, Grady CL (2010) Reliable differences in brain activity between young and old adults: A quantitative meta-analysis across multiple cognitive domains. Neurosci Biobehav Rev 34:1178–1194 Available at: http://dx.doi.org/10.1016/j.neubiorev.2010.01.009.

Taylor JR, Williams N, Cusack R, Auer T, Shafto MA, Dixon M, Tyler LK, Cam-CAN X, Henson RN (2015) The Cambridge Centre for Ageing and Neuroscience (Cam-CAN) data repository: Structural and functional MRI, MEG, and cognitive data from a cross-sectional adult lifespan sample. Neuroimage 144:262–269 Available at: http://dx.doi.org/10.1016/j.neuroimage.2015.09.018.

Tzourio-Mazoyer N, Landeau B, Papathanassiou D, Crivello F, Etard O, Delcroix N, Mazoyer B, Joliot M (2002) Automated anatomical labeling of activations in SPM using a macroscopic anatomical parcellation of the MNI MRI single-subject brain. Neuroimage 15:273–289.

Venables WN (William N., Ripley BD, Venables WN (William N). (2002) Modern applied statistics with S.

Wagenmakers E-J (2007) A practical solution to the pervasive problems of p values. 14:779–804.

West RL (1996) An application of prefrontal cortex function theory to cognitive aging. Psychol Bull 120:272–292.

Figures and Figure legends

Figure 1

Figure 2

Figure 3

Tables and Table legends

Table 1

Table 2